Violation of Vegard's law in covalent semiconductor alloys

C. Y. Fong,* W. Weber,† and J. C. Phillips
Bell Laboratories, Murray Hill, New Jersey 07974
(Received 21 June 1976)

Anomalous S-shaped deviations from Vegard's law in some semiconductor alloys are attributed to the effect of bond-bending forces. This idea is substantiated by numerical calculations on two-dimensional model alloys. A criterion is found which separates the occurrence of usually observed concave bowing and S-shaped deviations. In addition, our results show that the distribution of bond lengths in an alloy is bimodal.

I. INTRODUCTION

According to Vegard's law,[1] the lattice constants $a(x)$ of alloys should vary linearly with composition x. However, in pseudobinary semiconductor alloys $A_{1-x}B_xC$ (cation alloy) or $AC_{1-x}D_x$ (anion alloy) substantial violations of Vegard's law have been found[2-5] for which no physical explanation has been given.

In most alloys[4,5] the lattice constants bow below the corresponding linear value. Such quadratic deviations are always found in metallic alloys.[6] Surprisingly, some covalent pseudobinary alloys exhibit S-shaped (cubic) violations of Vegard's law,[2,3] as shown in the inset of Fig. 1(A). In this paper, we attribute the unusual cubic violation to the importance of bond-bending forces in the covalent alloys. Numerical calculations on model alloys will be presented to confirm this mechanism. Furthermore, our studies can elucidate the nature of disorder in these alloys.

In the following, we first give a qualitative description of the effect of the bond-bending forces (Sec. II). In Sec. III the method of our numerical calculations is displayed, and our results are presented and discussed in Sec. IV.

II. QUALITATIVE CONSIDERATIONS

To see qualitatively how bond-bending forces cause the S-shaped deviation, let us examine two extreme concentrations ($x \sim 0$ or 1) in the case of $AC_{1-x}D_x$. For small x, the bonds around the few substituted large size ions D tend to expand, which in turn will induce changes of the bond angles at neighbor ions. However, the bond-bending forces of the host lattice, provided that they are sufficiently large, will resist any distortion of angles and, thus, prevent the bonds around the ions D from expanding, so that the average lattice parameter of the alloy, $a(x)$, is smaller than Vegard's value. In the case of $x \approx 1$, i.e., when a few small ions C are substituted for the ions D, an analogous argument leads to values of $a(x)$ above the linear law. Therefore, the deviation will exhibit an S shape.

When, on the contrary, the bond-stretching forces are dominant, one always finds either a concave or convex curve for $a(x)$, depending on whether the force constant of AC is larger or smaller than that of AD; no S shape can be expected. This result can be easily verified by similar model considerations. As a consequence, we can explain the quadratic deviation from Vegard's law in metal alloys,[6] because bond stretching, or central forces are dominant in the densely packed metal structures.

III. DETAILS OF NUMERICAL CALCULATIONS

Let us turn to the discussion of the detailed calculations on model alloys which contain ~100 atoms in a periodically repeated two-dimensional unit cell. Two structures have been studied—the square (SL) and the trigonal (TL) boron-nitride lattices. The pseudobinary alloy is simulated by randomly substituting the ions at one sublattice to the extent specified by the composition x.

We have used Keating's potentials[7] for the harmonic bond stretching, purely noncentral bond-bending and the anharmonic bond-stretching forces, which have been found to be the most important contributions.[8,9] Both Coulomb interaction and the anharmonic bond-bending forces have been neglected.[10,11]

The potential energy at any ion 0 is given by

$$V = \frac{1}{2}\sum_{i=1}^{N_k}\frac{\alpha_{0i}}{(\eta_k)^2}(\vec{\mathrm{x}}_{0i}\cdot\vec{\mathrm{x}}_{0i} - X_{0i}^2)^2 + \frac{1}{3!}\sum_{i=1}^{N_k}\frac{\gamma_{0i}}{(\eta_k)^3}(\vec{\mathrm{x}}_{0i}\cdot\vec{\mathrm{x}}_{0i} - X_{0i}^2)^3 + \frac{1}{2}\sum_{i>j}^{N_k}\frac{\beta_{i0j}}{\eta_k'^2}(\hat{x}_{0i}\cdot\hat{x}_{0j} - \hat{X}_{0j}\cdot\hat{X}_{0j})^2 , \quad (1)$$

where α_{0i}, γ_{0i} are the harmonic and anharmonic bond-stretching force constants between the center ion 0 and its ith neighbor. The bond-bending force

parameter β_{i0j} depends on the sort of ion 0. Because of the heteropolarity, one expects that $\beta_{ACA} \neq \beta_{CAC}$, etc. In the following, we define[8] $\beta_{AC} = \frac{1}{2}(\beta_{ACA} + \beta_{CAC})$, and $C \to D$ for compound AD. N_k is the number of the nearest neighbor, with $k = 1, 2$ for the SL and the TL. η_k and η'_k are normalization factors. Finally $\vec{x}_{0i}$ is the distance vector from ion 0 to the ith neighbor and X_{0i} is the equilibrium bond length of the corresponding pure compound.

With a set of force parameters and equilibrium bond lengths the lattice constant of the alloy $a(x)$ is determined by a relaxation method involving the following steps: (i) assigning five virtual lattices with two lattice constants larger than, two smaller than, and one equal to the value predicted by Vegard's law; (ii) letting each ion in a virtual lattice relax according to $dV/d\vec{x}_0 = 0$, where $\vec{x}_0$ is the position vector of the ion measured with respect to an origin in the unit cell and V is given in Eq. (1); (iii) calculating the total energy; (iv) iterating (ii) and (iii) until the lattice relaxes to the lowest total energy; and (v) fitting the five energies with a parabola to find $a(x)$ corresponding to the minimum energy.

The force constants span a multidimensional parameter space which is difficult to explore completely. However, it is not necessary to do so, since we have guidelines for typical values of α, β, and γ from studies of the elastic properties in zinc-blende[8] (ZB) and diamond-type[9] crystals. The sets of parameters separating the concave and the S-shaped deviations for the two lattices are listed in Table I along with the equilibrium bond length; α, β, and γ given in Refs. 8, 9, and 12.

IV. RESULTS AND DISCUSSION

All values of our parameters for the trigonal lattice are close to those of the three-dimensional ZB materials. A similar S-shaped curve for the square lattice required, however, values of the β/α ratio to be $\approx 30\%$ larger, and of the γ's $\approx 50\%$ smaller than the corresponding ZB numbers. Furthermore, the maximum values of $\Delta a(x)100/a$ are ≈ 0.07 (TL) and 0.04 (SL), whereas in ZB materials the typical deviations are 0.1–0.2.[2-4] The discrepancy between the trigonal and ZB cases may be due to the difference in dimensionality. This argument does not seem to apply for the much smaller value of the SL. Also, the SL force constants which yield S-shaped curves lie outside the physically realistic range. This suggests that the SL is not very well suited to simulating an open structure in two dimensions.

Relations among the force constants have been examined near the special points in parameter space given in Table I. As $\alpha_{AD}/\alpha_{AC} \to 1$, β/α for each compound can be reduced. This is consistent with the above qualitative discussion. An increase of γ or of the asymmetry in β will enhance the S-shaped violation.

The most sensitive quantity for the separation between S-shape and concave curves is the difference in the bond bending forces of the two constituents. To demonstrate this most clearly, we express the deviation from Vegard's law by

$$\Delta a(x) = C_2 x(1-x) + C_3(2x-1)x(1-x) . \qquad (2)$$

C_2 and C_3, characterizing the strengths of the quadratic and cubic deviations, are determined by

TABLE I. Parameters for the trigonal and square lattices. Distances are given in Å; α, β, and γ in 10^3 dyn/cm and 10^{11} dyn/cm^2. Also given are typical values for III-V compounds. Numbers in brackets denote ZB (three-dimensional) values for γ and β/α, appropriately scaled to account for differences in dimensionality, normalization, and bond angles.

	SL	TL	ZB
X_{AC}	2.637	2.637	2.36–2.804[a]
X_{AD}	2.806	2.806	
α_{AC}	37.5	37.5	37.8[a]
α_{AD}/α_{AC}	0.856	0.86	0.86[a]
γ_{AC}	−99.52 } (−187)	−187.06 } (−225)	−187[b]
γ_{AD}	−69.32 }	−170.33 }	
β_{AC}	14	14.67	7.13[a]
β_{ACA}/β_{CAC}	1.33	2	1.5–2[c]
β_{ADA}/β_{DAD}	1.42	1.21	
β/α	0.37(0.293)	0.39(0.39)	0.195[a]
β_r^{cr}	−0.059	−0.068	−0.071

[a] Data are taken from Ref. 8.
[b] Data are taken from Ref. 9 (for Ge).
[c] Data are taken from Ref. 12.

a least-squares fit to Δa at four different compositions. In Figs. 1(A) and 1(B), C_2 and C_3 are plotted versus $\beta_r=(\beta_{AD}-\beta_{AC})/(\beta_{AD}+\beta_{AC})$. The vertical arrows indicate the values of β_r^{cr}, where $\Delta a(x=0.8)>0$, separating sets of concave $a(x)$ curves on the left and S-shaped $a(x)$ curves on the right of β_r^{cr}. We choose $x=0.8$ as a proper indicator for definiteness of the separation, in view of both numerical convergence problems and experimental uncertainties near $x\approx 0$ or $x\approx 1$. Mathematically, however, an S-shaped $a(x)$ curve will exist as long as $|C_3|\approx|C_2|$. For small β_{AD}; e.g., for $\beta_r<\beta_r^{cr}$, the harmonic bond-stretching forces prevail and cause the concave deviation. On the other hand, for $\beta_r>\beta_r^{cr}$, the stiffness of the bond angles tries to maintain the bond length close to X_{AD}, thus producing the S-shaped violation.

In real ZB alloys, β_r also seems to be the physical quantity which separates the two kinds of violations. To our knowledge, all materials with $\beta_r\geq -0.071$ show S shape, whereas concave deviations are only found[4,5] for $\beta_r<-0.071$; the β values of the constituents are taken from Ref. 8.

The static disorder of the alloy ions away from their ideal lattice sites is given by the static root-mean-square displacement $\bar{u}$. This quantity is the static contribution to the Debye-Waller factor in our alloy, and could be obtained by careful x-ray diffraction studies. For $x=0.8$ and $\beta_r=-0.06$ we find $\bar{u}=\langle\frac{1}{2}\vec{u}^2\rangle^{1/2}=0.04, 0.05$ Å for the square and trigonal lattice, respectively. These numbers compare favorably with the one obtained by a one-dimensional hard-sphere model,[13] where

$$\bar{u}_{hs}=\tfrac{1}{2}[x(1-x)]^{1/2}|X_{AC}-X_{AD}|=0.034\ \text{Å}. \qquad (3)$$

The nature of the disorder effect in the ZB alloys can be illustrated by the distribution functions of the bond angles and bond lengths. The bond angles form unimodal distributions around the equilibrium angles of 120° and 90°; the widths are 4° and 2° for the TL and the SL, respectively. However, the distributions of the bond length are bimodal in both lattices. We plot the distribution functions in Figs. 2(A) and 2(B). The peaks of the TL are better separated than the ones in SL, and the maxima of the TL peaks lie closer to the bond lengths of the constituents. The line shapes of all peaks are in general close to Gaussian, e.g., the quotient $\langle(\Delta r)^4\rangle/[3\langle(\Delta r)^2\rangle^2]=0.89$, 0.79, 0.97, and 1.32 for the minor, major peaks of the TL and the SL, respectively, whereas the ideal value is 1. These moments were calculated with respect to appropriate peak positions. The linewidths for the structures in TL are nearly equal to (0.04 Å) whereas in SL, the ones for the minor and the major peaks are 0.045 and 0.055 Å.

All the features discussed above depend neither strongly on x nor critically on the particular set of force parameters. The difference between the

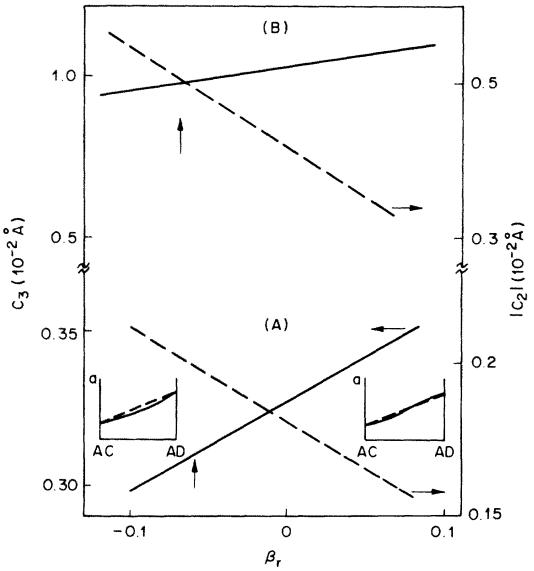

FIG. 1. Dependence of the coefficients C_2 (dashed lines) and C_3 (full lines) on β_r : (A) square lattice, (B) trigonal lattice. The vertical arrows indicate β_r^{cr} separating concave and S-shaped $a(x)$ curves. The two insets indicate the two characteristic violations.

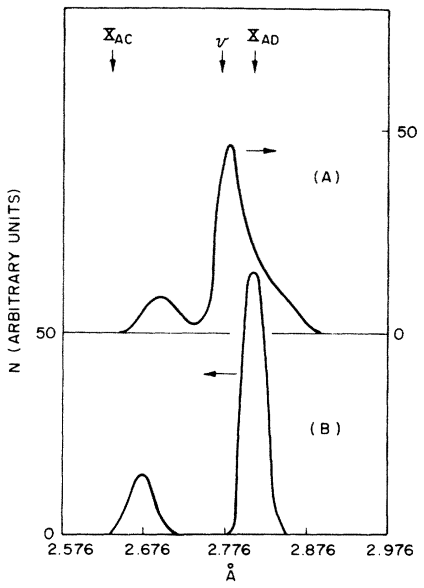

FIG. 2. Distribution functions for the bond lengths: (A) square lattice, (B) trigonal lattice. The two curves are smoothed from histograms. X_{AC}, X_{AD} and v indicate, respectively, the equilibrium bond lengths and Vegard's value.

TL and SL is probably due to the fact that the TL is less densely packed, therefore it is easier for the ions to maintain their "natural" bond lengths, which in turn, induces a larger spread of the distribution in bond angles.

In the treatment of alloy problems, it is usually assumed that the atoms are located at the ideal lattice sites. For example, in the virtual-crystal approximation,[14] an averaged atomic separation is used as well as an averaged periodic potential. Similarly in treating phonons in the binary alloys, the random-element isodisplacement,[15] takes into account the differences in the force constants and the ionic masses in an averaged way. The improvement achieved by the coherent-potential approximation[16] is only to account for the potential fluctuations of the alloy constituents around the average potential, but not to take lattice relaxation into account.

There is, however, much evidence that the effects of relaxation in alloys cannot be simply neglected. This may, e.g., be seen from calculations of impurity-state energies in semiconductors[17] and also from calculations of surface states in semiconductors which agree with experiment only when relaxation is taken into account.[18] Furthermore, CPA calculations on electronic density of states for semiconductor alloys[16] lead to band tails in the gap region, which is a qualitatively wrong feature of the approach, as no band tails are observed experimentally.[19,20] Similarly in properly prepared samples of amorphous semiconductors no band tails have been found.[21] It has been argued that "lattice relaxation" leads to the vanishing of the band tails.[22] Also, it has been shown that surface relaxation leads to the shift of occupied surface states in the bulk gap toward the bulk valence band and of unoccupied surface states toward the bulk conduction band.[23]

Our calculations, for the first time, take into account lattice relaxation in alloys. We arrive at an important result that the distribution of the bond lengths is bimodal, rather than unimodal, which would be more consistent with the virtual-crystal[14] or coherent-potential[16] approaches. This bimodal distribution of bond lengths should be incorporated in refined treatments of semiconductor alloy problems. As a first step, this could be accomplished by using two weighted Gaussian distributions located about the natural bond lengths with a width of approximately $\frac{1}{4}|X_{AC} - X_{AD}|$.

In conclusion, we attribute the physical origin of the anomalous S-shaped violation of Vegard's law in semiconductor alloys to covalent bond-bending forces. To confirm this assumption we have performed numerical calculations of the lattice constant $a(x)$ for various compositions x in two-dimensional pseudobinary model alloys, using harmonic and anharmonic potentials of Keating type. The difference in the bond-bending forces of the two constituents turns out to be the critical quantity for separating the normally observed concave $a(x)$ from the s-shaped curves. Our calculations also allow conclusions on the disorder effects in alloys. We find unimodal distributions for bond angles, yet bimodal ones for the bond lengths, all of approximately Gaussian form. The bimodal distribution is more pronounced for more open crystal structures. Finally, our method for calculating lattice relaxation is easily applicable to three-dimensional alloy systems and could also be extended to calculate electronic and vibrational properties.

---

*On leave of absence from University of California, Davis, Calif.

†On leave of absence from Max-Planck-Institut für Festkörperforschung, Stuttgart, West Germany.

[1]L. Vegard, Z. Phys. 5, 17 (1921).

[2]O. V. Bogorodskii, A. Ya. Nashel'skii, and V. Z. Ostrovskaya, Sov. Phys.-Crystallogr. 6, 95 (1961).

[3]J. C. Woolley and J. Warner, J. Electrochem. Soc. 111, 1142 (1942).

[4]J. C. Woolley and B. Ray, J. Phys. Chem. Solids 13, 151 (1960).

[5]E. K. Muller and J. L. Richards, J. Appl. Phys. 35, 1233 (1964).

[6]W. B. Pearson, *A Handbook of Lattice Spacing and Structures of Metals and Alloys* (Pergamon, London, 1958), Vol. 1.

[7]P. N. Keating, Phys. Rev. 145, 637 (1966).

[8]R. M. Martin, Phys. Rev. B 1, 4005 (1970).

[9]P. N. Keating, Phys. Rev. 149, 674 (1966).

[10]J. Noolandi, Phys. Rev. B 10, 2490 (1974).

[11]J. A. Van Vechten, Phys. Rev. B 10, 4222 (1974).

[12]K. C. Rustagi and W. Weber, Solid State Commun. 18, 673 (1976).

[13]P. D. Dernier, W. Weber, and L. D. Longinotti (unpublished).

[14]L. Nordheim, Ann. Phys. (Leipz.) 9, 607 (1931); 9, 641 (1931).

[15]G. Lucovsky, K. Y. Cheng, and G. L. Pearson, Phys. Rev. B 12, 4135 (1975), and references therein.

[16]D. Stroud and H. Ehrenreich, Phys. Rev. B 2, 3197 (1970); E-Ni Foo and M. Ausloos, J. Noncryst. Solids 8-10, 134 (1972).

[17]A. Baldereschi and J. J. Hopfield, Phys. Rev. Lett. 28, 171 (1972).

[18]J. A. Appelbaum and D. R. Hamann, Phys. Rev. Lett. 31, 106 (1973); 32, 225 (1974).
[19]J. C. Woolley, M. B. Thomas, and A. G. Thomson, Can. J. Phys. 46, 157 (1968).
[20]See also discussion of this point by J. A. Van Vechten and T. K. Bergstresser, Phys. Rev. B 1, 3351 (1970).
[21]W. E. Spicer, T. M. Donovan, and J. E. Fischer, J. Noncryst. Sol. 8-10, 122 (1972); G. A. N. Connell, Solid State Comm. 14, 377 (1974).
[22]J. C. Phillips, Comments on Solid State Phys. 4, 9 (1971).
[23]M. A. Schluter, J. R. Chelikowsky, S. G. Louie, and M. L. Cohen, Phys. Rev. Lett. 34, 1385 (1975); K. C. Pandey and J. C. Phillips, Phys. Rev. Lett. 34, 1450 (1975); J. A. Appelbaum and D. R. Hamann, Phys. Rev. B 12, 1410 (1975); W. A. Harrison, Surf. Sci. 55, 1 (1976).